Experiments in Fluids 27 (1999) 332–338 © Springer-Verlag 1999

Capillary wave gas exchange in the presence of surfactants

J. R. Saylor, R. A. Handler

Abstract The effect of surfactants on gas exchange across an air/water interface populated with capillary waves, is considered. Experiments were conducted on capillary waves having a wavelength of 2.87 mm in the presence of oleyl alcohol and stearic acid, as well as on surfaces which were surfactant-free. The presence of these surfactants decreased the gas exchange rate by at most a factor of two when the energy delivered to the tank was held constant. Thus, even in the presence of surfactants, pure capillary waves still caused significant gas exchange, indicating that partially damped capillary waves may play an important role in air/sea gas exchange. When the gas exchange coefficient was plotted as a function of mean square slope, the presence of surfactants was found to negligibly affect the gas exchange rate, with the possible exception of the high wave slope regime for stearic acid. This result suggests that it is principally the kinematics of wave motion which accounts for the enhancement of transport due to the capillary waves investigated here. Moreover, these results agree with those obtained from polychromatic, wind-generated waves, suggesting that, for non-breaking waves, knowledge of the statistics of the wave field may be all that is required to parameterize the gas exchange coefficient.

1 Introduction

The transport of heat and mass across an air/water interface has many environmental implications including global warming, weather prediction, and the ultimate fate of pollutants. The physical processes which occur at the air/water interface determine the rate at which heat and mass transport occurs. Processes such as turbulence, wave generation and breaking, bubble formation and droplet generation all affect transport. Many of these processes have been studied in considerable detail to ascertain their ability to enhance the transport of heat and dissolved gasses across an air/water interface.

Received: *10 June 1998/Accepted*: *3 November 1998*

J. R. Saylor, R. A. Handler
Naval Research Laboratory, 4555 Overlook Av. SW
Washington DC 20375-5351, USA

Correspondence to: J. R. Saylor

The authors would like to thank William R. Barger for providing the data presented in Fig. 2, as well as for his enormously helpful advice and suggestions. Financial support was provided by the Office of Naval Research through the Naval Research Laboratory, and the National Research Council.

One physical process which occurs at the air/water interface, and which has not received a significant amount of experimental attention is capillary waves. Theoretical studies of capillary waves using an exact solution due to Crapper (1957) were performed by Witting (1971) for heat transfer, which predicted significant enhancements. Szeri (1997) performed an analysis for gas exchange and also noted significant transport enhancements due to capillary waves; furthermore Szeri noted that it is the straining of the fluid in the trough of these waves and the concomitant stretching of the concentration boundary layer which was responsible for this enhanced transport. In spite of these theoretical results, experimental studies are lacking. Typical gas exchange experiments utilize wind/wave tunnels, where a gas exchange coefficient K is correlated to a wind speed u. Capillary waves exist in such studies, but they are accompanied by many other physical phenomena such as wave breaking and turbulence which prevent one from ascertaining the role that capillary waves play in transport. In numerous wind/wave tunnel experiments, K has been observed to increase much more rapidly with u when a critical wind speed is exceeded (Ocampo-Torres et al. 1994; Kanwisher 1963; Broecker et al. 1978; Downing and Truesdale 1955; Hoover and Berkshire 1969; Liss 1973; Jähne et al. 1979); moreover, in many of these studies it was noted that capillary waves are observed to first form at this critical wind speed, suggesting the possible importance of capillary waves in gas exchange.

In spite of these results which suggest an important role for capillary waves, very little experimental work has been done to isolate capillary waves and determine their role in gas exchange. MacIntyre (1971) studied gas exchange due to capillary waves created by acoustically exciting a flask with a loudspeaker, while simultaneously stirring the liquid bulk. These experiments indicated a modest increase in transport by the capillary waves, but interpretation of the results is complicated by a lack of information concerning the stirring. Saylor and Handler (1997) used Faraday waves (Faraday 1831) to isolate and control capillary waves and ascertain their role in carbon dioxide transport. Faraday waves are created by vibrating a tank of water in the vertical direction, generating a uniform field of waves at one-half the excitation frequency. These experiments demonstrated that capillary waves can have a significant effect on gas exchange rates, increasing that rate by almost two orders of magnitude over that which is obtained from a flat surface. However, these experiments were all conducted for the case of a clean water surface, while the ultimate goal of gas exchange research is to predict gas exchange rates on the larger scale of oceans and lakes which are

almost always surfactant-influenced. Consequently, the work of Saylor and Handler (1997), while useful in illustrating how gas exchange by capillary waves is affected by the wavelength and wave slope, is limited in the sense that a surfactant-free water surface is uncommon in nature. The work presented herein addresses the need to ascertain the behavior of surfactant-covered capillary waves in the gas exchange process.

The ability of surfactants to damp waves is well-known, and numerous studies have been published documenting this phenomenon. Reviews of this work are provided in the texts of Gaines (1966) and Adamson (1990). The effectiveness of surfactants in damping capillary waves notwithstanding, it is important to note that capillary waves can still exist in the presence of surfactants. Furthermore, it is unclear whether such waves will behave the same as their clean counterparts, all other things being equal. In other words, the main question which we seek to address herein is the following: do two capillary waves of identical slope and wavelength provide the same gas exchange potential if one wave is clean and the other is covered with a surfactant monolayer?

A secondary motivation for this research is to shed some light on the parameterization of the gas exchange coefficient K. Jähne et al. (1987) suggested that independent of experimental facility and conditions, K should be well parameterized by the mean square slope for the wave field, $\overline{S^2}$. They also presented data in support of this notion (although plots of K versus $\overline{S^2}$ were not provided). This is an important idea, since parameterization of K by such quantities as wind speed or friction velocity show significant variations from facility-to-facility, and also with the degree and type of surfactant contamination. Although considerable time has passed since Jähne et al. (1987) suggested this parameterization, very little experimental evidence has been presented in support of this approach. To the author's knowledge, the only other data which has been presented in support of this notion is that of Frew (1997), who correlated K to $\overline{S^2}$ in a wind/wave tunnel study, for clean surfaces and surfaces contaminated by three different surfactants. The data show an excellent linear correlation of K to $\overline{S^2}$, independent of surfactant concentration or type, and with very little scatter. This is a remarkable result in that it suggests the gas exchange coefficient can be predicted from knowledge of the wave surface topology alone (for non breaking waves). In addition to simplifying the analysis of gas exchange, these results are also important in that $\overline{S^2}$ of the ocean surface is more directly obtainable from optical or radar-based remote sensing methods than other parameters such as wind speed or friction velocity.

The data presented by Frew (1997) were obtained using a wave slope gauge having a resolution of 1200 rads/m ($\lambda = 5$ mm) (Frew 1998). While the resolution of these measurements is high, it is important to note the possibility that the computed value of $\overline{S^2}$ may change as the resolution is increased still further. Recent work due to Saylor (1998) suggests that the contribution of capillary waves to gas exchange peaks at wavelengths near $\lambda = 3$–4 mm. Hence, it is desirable to obtain information on capillary waves a bit smaller than those resolved in the work of Frew (1997). In the current work, waves having a wavelength $\lambda = 2.87$ mm are investigated, and the slopes of these waves are fully resolved. One important aspect of these experiments is that the degree of success in parameterizing K by $\overline{S^2}$ for the waves considered is indicative of how well such a parameterization should be expected to work for higher resolution wind/wave tunnel or oceanic studies.

The capillary waves which were investigated in this work were Faraday waves. A review of the theory of these waves can be found in Miles and Henderson (1990). Faraday waves differ from the capillary waves which exist on the ocean in that they are not progressive waves and are generated by a different driving force. While it is desirable to perform laboratory experiments on waves which are as similar as possible to those which exist on the ocean, this is not possible for small-scale capillary waves for the following reasons. Generation of such waves via wind shear inevitably is accompanied by turbulence and results in a polychromatic wave field, preventing one from isolating the capillary waves and their effect on gas exchange. Moreover, generation of waves using a mechanical dipper or paddle is also not feasible since capillary waves of the size considered here decay too rapidly to permit the creation of a uniform wave field of any appreciable extent. For these reasons, Faraday waves represent the best platform for studying the transport properties of capillary waves.

The paper is organized as follows. The experimental method is described in Section 2, followed by the presentation of results in Sect. 3. The significance of these results is discussed in Sect. 4, followed by a summary in Sect. 5.

2 Experimental method

The experimental apparatus used in these experiments is presented in Fig. 1. A $5'' \times 5''$ plexiglass tank was mounted on an electrodynamical shaker which was driven at a user-defined amplitude. The excitation frequency f used for all experiments was 280 Hz, resulting in Faraday waves having a frequency $f_w = 140$ Hz. The wavelength of these waves was computed using the linear dispersion relationship (Dietrich 1963)

$$c^2 = \left\{ \left(\frac{g\lambda}{2\pi} \right) \left[\frac{(\rho - \rho')}{\rho} \right] + \left[\frac{\sigma}{(\rho + \rho')} \right] \left(\frac{2\pi}{\lambda} \right) \right\} \tanh h \left(\frac{2\pi}{\lambda} \right) h \qquad (1)$$

where c is the phase speed of the wave, σ is the surface tension, g the gravitational acceleration, λ the wavelength, ρ the water density, ρ' the air density, and h the water height. The value of λ was obtained by substituting $c = \lambda f_w$ in the left hand side and then solving for λ. For $f_w = 140$ Hz and using the surface tension value for a clean water surface (0.0718 N/m), one

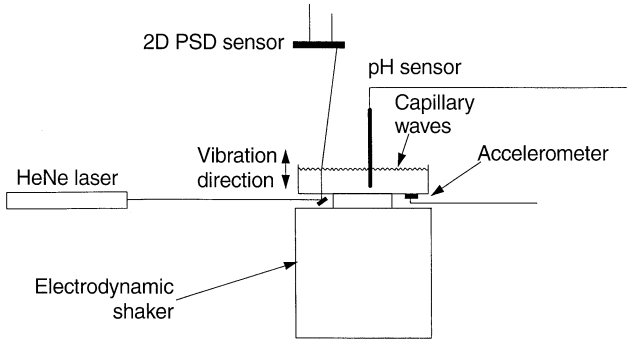

Fig. 1. Schematic illustration of experimental setup

obtains $\lambda = 2.87$ mm. The value of σ in Eq. (1) was reduced when surfactants were introduced. For the experiments presented here, the presence of surfactants reduced σ to 0.0668 N/m, resulting in a computed value of $\lambda = 2.82$ mm, which is a 2% reduction from the clean value. This difference is negligible for the present purposes and the clean value is used hereinafter.

Prior to each experiment, the water surface was vacuumed using a peristaltic pump. The remaining water was then aspirated from the tank, and the tank was cleaned by rinsing with copious amounts of distilled water. In between runs where surfactants were used, the tank was periodically cleaned with HPLC grade heptane followed by cleaning with dilute reagent grade methanol, and then several distilled water rinses. The working fluid for all experiments was distilled water.

An accelerometer was mounted on the water tank in a direction parallel to the shaker motion. The signal from the accelerometer was digitized and recorded by the computer controlled data acquisition system. The accelerometer output was a sine wave, which characterizes the energy being delivered to the tank in a given experiment. The amplitude of this sine wave g_p was computed as

$$g_p = \sqrt{2}\, g_{\mathrm{rms}} \tag{2}$$

where g_{rms} is the root mean square of the entire accelerometer time trace. This procedure was used, instead of setting g_p to the maximum value in the accelerometer time trace, to avoid sensitivity to possible spurious values in the accelerometer data.

2.1 Wave slope measurement

The wave slope was measured using a laser slope gauge which is illustrated in Fig. 1. A HeNe laser beam was directed vertically upward through the floor of the plexiglass tank. The optics were adjusted so that the beam was focussed at the water surface, achieving a beam diameter less than 180 μm for the experiments presented here. Using the criterion of Cox (1958), this beam diameter is more than adequate to resolve wave slopes for the 2.87 mm waves investigated. When the beam passed through the air/water interface, it was refracted by the angled surface of the water wave. The refracted beam was detected by a position sensitive detector (PSD). The PSD output consists of two voltages which are linearly related to the position at which the laser strikes the detector. Using Snell's law and trigonometry, the PSD output was converted into an instantaneous wave slope $S(t)$. Data from the PSD was acquired by the data acquisition system, and at the conclusion of an experiment this data was compiled and the mean square slope $\overline{S^2}$ was computed. Further details of the wave slope measuring system including the calibration method can be found in Saylor and Handler (1997).

2.2 Measurement of K

A time-trace of the CO_2 concentration in the tank was obtained for each experiment using a pH meter and subsequently converting the measured pH values to carbon dioxide concentrations $[CO_2]$. The conversion of pH to $[CO_2]$ was achieved using the equations for the chemical equilibrium of CO_2 in water (Stumm and Morgan 1970). Prior to each experiment, CO_2 was bubbled into a flask of distilled water. When this water approached saturation, 300 ml was transferred into the plexiglass tank. The pH electrode was then inserted beneath the water surface. For the surfactant runs, a monolayer of surfactant was applied to the water surface at this point, using the procedure described below. The electrodynamic shaker was then turned on and data acquisition initiated. Prior to each experiment, a two-point calibration of the pH electrode was performed using buffer solutions at a pH of 4 and 7.

Once the experiment was complete, the CO_2 time trace was converted to a gas exchange coefficient K, using the equation

$$\frac{\partial C_w}{\partial t} = \frac{-K}{h}\left(C_w - \frac{C_a}{H}\right) \tag{3}$$

where C_w is the concentration of CO_2 in the water, C_a is the concentration of CO_2 in the air, h is the height of the water, and H is the Henry's law constant which accounts for the degree of solubility of $[CO_2]$ in the water. Integrating Eq. (3) over time gives

$$C_w = \left(C_{w,0} - \frac{C_a}{H}\right) \mathrm{e}^{(-K/h)t} + \frac{C_a}{H} \tag{4}$$

where t is time and $C_{w,0}$ is the concentration at $t = 0$. Assuming the hydrodynamics do not change during the course of an experiment, Eq. (4) requires that the C_w versus t data yield a straight line of slope $-K/h$, when plotted on semi-logarithmic coordinates. Values for K were obtained by performing a least squares fit to the time traces of log $[CO_2]$.

2.3 Surfactant application

Experiments were conducted for water surfaces which were (i) surfactant-free, (ii) covered with a monolayer of stearic acid (Aldrich, 99 + % purity) and (iii) covered with a monolayer of oleyl alcohol (white, Hormel Institute). For the surfactant experiments, stock solutions of each surfactant were prepared using HPLC grade heptane. Drops of this solution were then applied to the water surface in ~10 μl increments using a micrometer syringe. These drops formed small liquid heptane lenses which subsequently evaporated, leaving a monolayer of the dissolved surfactant on the water surface. After deposition of the monolayer, the shaker was energized and data acquisition initiated.

Surface pressure Π versus surface concentration c plots are presented in Fig. 2 for stearic acid and oleyl alcohol to illustrate the difference in behavior of the two surfactants. As Fig. 2a shows, Π changes very rapidly with c for stearic acid for all but very small values of c. Hence, reproducing the same value of Π from run-to-run is difficult for stearic acid, since small errors in the mass deposited translate to large variations in Π. To avoid this problem an excess of stearic acid was deposited onto the surface to insure that Π was equal to the equilibrium spreading pressure Π^e, a thermodynamic quantity which is not expected to vary significantly under the laboratory conditions for which these experiments were conducted. Upon complete evaporation of heptane from the deposited heptane/stearic acid lenses, small particles formed on the water surface, which were

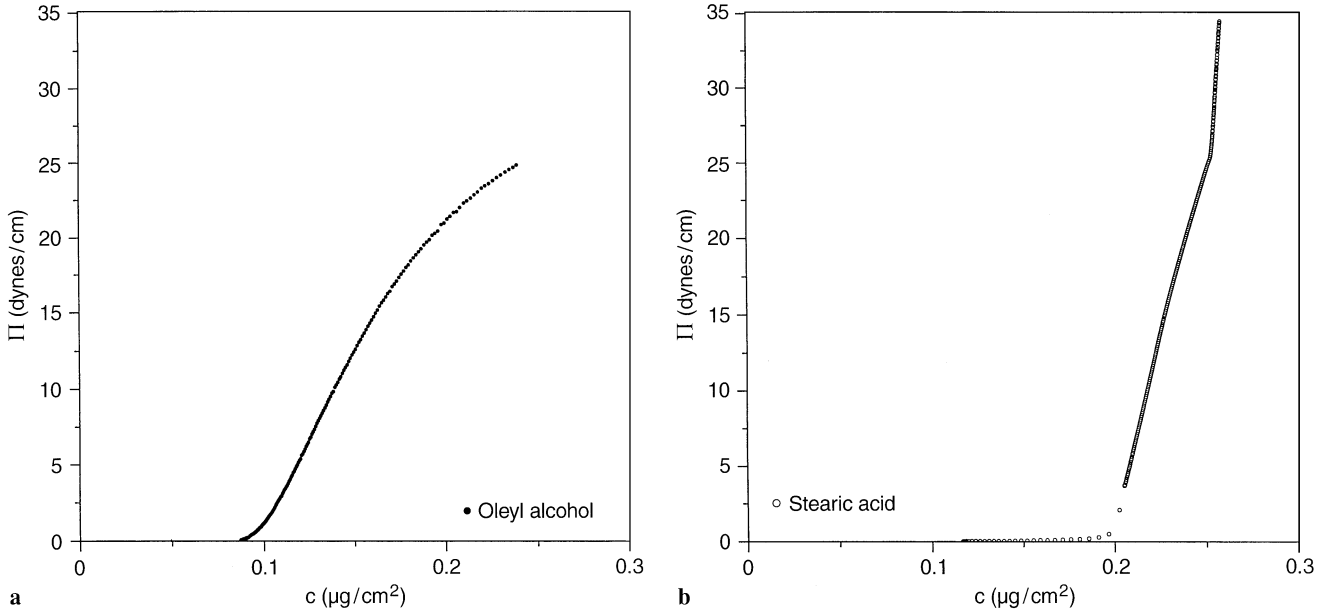

Fig. 2. Π versus c for **a** oleyl alcohol and **b** stearic acid. Data obtained from Barger (1998)

assumed to be small stearic acid crystals, indicating that the monolayer was indeed in equilibrium with its bulk phase, and therefore $\Pi = \Pi^e$. No particles were observed upon evaporation of heptane from heptane/oleyl alcohol lenses.

For stearic acid on water $\Pi^e = 5$ dyn/cm (Gaines 1966), which is less than the maximum value of Π plotted in Fig. 2b. This is because the data in Figs. 2a and b were obtained in a Langmuir trough where pressures in excess of Π^e can be obtained by compression of the surface film with the trough barriers. For the experimental arrangement used here, Π^e is the maximum value of Π which can be obtained.

The oleyl alcohol experiments were run at the same surface pressure as for the stearic acid runs so that differences in the results could be related to the difference in the phase of the two surfactants (solid and liquid for stearic acid and oleyl alcohol, respectively), and not to differences in Π. Since Π^e for oleyl alcohol is greater than that for stearic acid, a value of $\Pi = 5$ dyn/cm was obtained by depositing the appropriate amount of surfactant on the surface. Referring to Fig. 2a a concentration $c = 0.12$ μg/cm^2, was deposited to yield the desired value. Controlling Π for oleyl alcohol was less delicate than for stearic acid since, the Π versus c curve is not as steep for oleyl alcohol.

The stearic acid and oleyl alcohol runs were identical in all regards except that the method of mounting the plexiglass tank was slightly different for the oleyl alcohol runs. For these runs, four 1/8″ thick rubber dampers were inserted between the plexiglass tank and the rigid mounting bracket which connected it to the electrodynamic shaker. The purpose of these dampers was to test for the presence of acoustic sources of CO_2 transport, such as acoustic streaming. It was noted that without these rubber dampers, audible acoustic radiation was emitted from the tank at high values of g_p. To investigate the possibility that this acoustic energy might contribute to gas exchange, the rubber dampers were inserted. These dampers audibly decreased the acoustic energy emitted from the tank. As will be described in Sect. 3, this had only a slight affect on gas exchange. However, in order to compare surfactant and clean runs under exactly the same experimental conditions, a set of clean (no surfactant) runs were obtained with these dampers in place. Thus, in the plots of K versus $\overline{S^2}$ presented in the next section, comparison of clean and surfactant data is always done for data sets obtained under identical experimental conditions.

3 Results

A plot of K versus g_p is presented in Fig. 3 for the stearic acid and clean data sets. The data presented in this figure was averaged in bins having a width of 0.1 g, so each point represents the average of several experiments. The rate of CO_2 transport is significantly diminished by the presence of the stearic acid monolayer. The difference between the two data sets exceeds a factor of two for large values of g_p. This result is in agreement with the well-known damping of capillary waves by surfactants. The stearic acid data exhibits a larger degree of scatter when compared to the clean data set (as well as when compared to the oleyl alcohol data presented later). A possible reason for this is described in the following section.

Extrapolating the data presented in Fig. 3 (and in Fig. 5, below) reveals a non-zero value for the x-intercept. This is due to the fact that Faraday waves require a finite acceleration before wave onset. Hence, at the x-intercept, the water surface is free of waves, even though $g_p \neq 0$.

In order to determine how gas exchange is affected by the presence of surfactants at constant wavelength and wave slope, the data of Fig. 3 is replotted as a function of $\overline{S^2}$ in Fig. 4. In this figure, the two data sets collapse (within the scatter) for wave slopes between zero and roughly 0.06 m/m. For $\overline{S^2} > 0.06$ m/m, the data sets seem to diverge, giving larger values of K for the clean case. It is noted, however, that this occurs only for the last few data points and that the difference is not much larger than

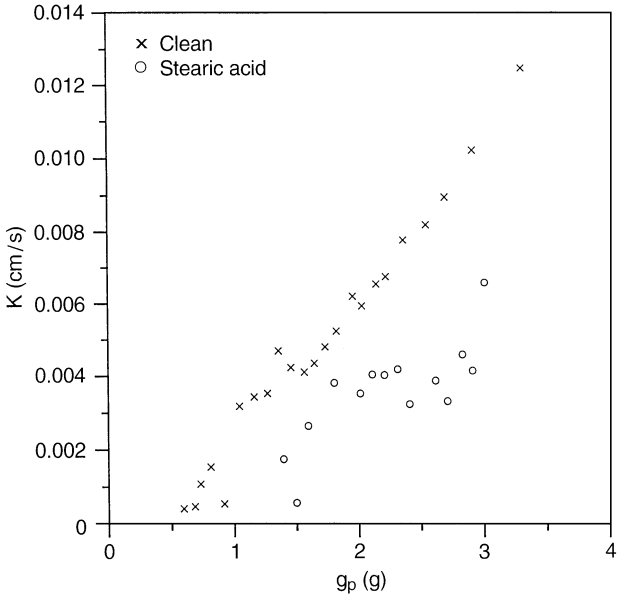

Fig. 3. K versus g_p for clean and stearic acid monolayer interfaces

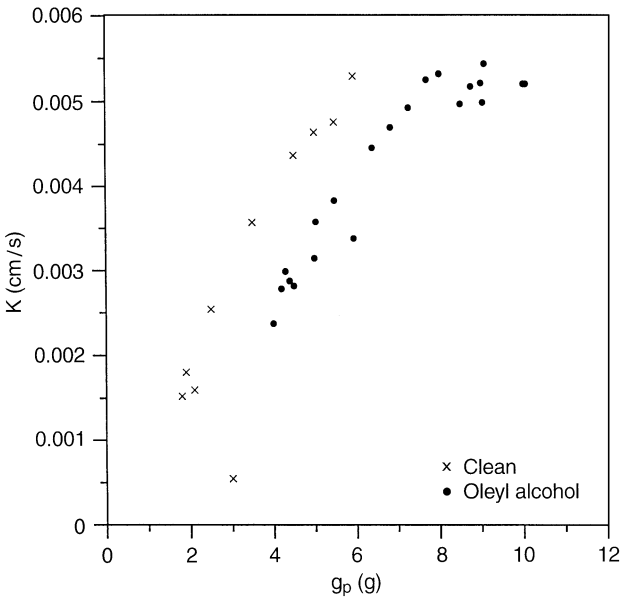

Fig. 5. K versus g_p for clean and oleyl alcohol monolayer interfaces

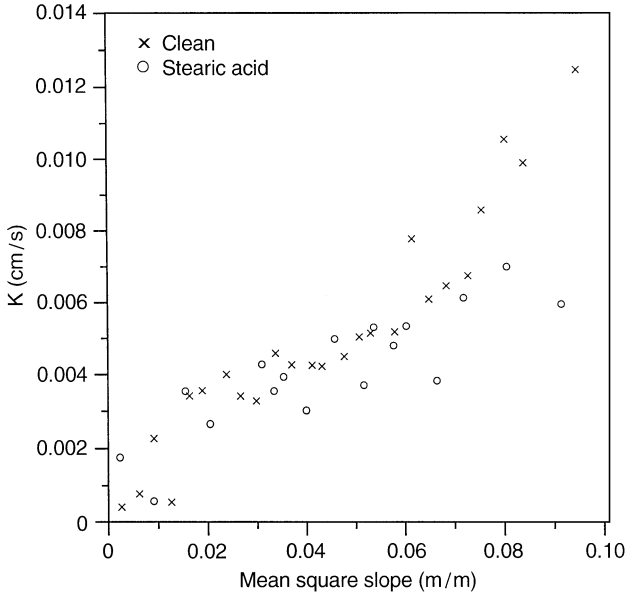

Fig. 4. K versus $\overline{S^2}$ for clean and stearic acid monolayer interfaces. Data averaged in bins of 0.0035 m/m width

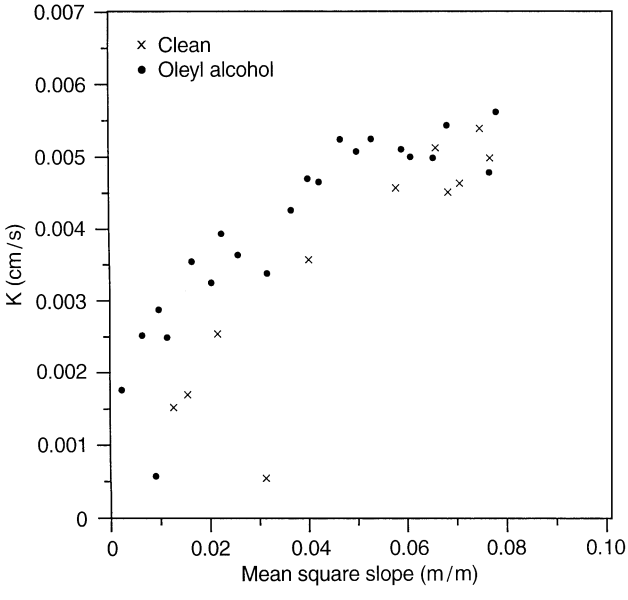

Fig. 6. K versus $\overline{S^2}$ for clean and oleyl alcohol monolayer interfaces. Data averaged in bins of 0.0035 m/m width

the scatter. For the purposes of this work, these two data sets are considered to fall on the same line.

The results for experiments conducted using oleyl alcohol as a surfactant are presented in Figs. 5 and 6. In Fig. 5, K is plotted as a function of g_p where, again, the data has been averaged in bins 0.1 g in width. This data is similar to that for stearic acid in that there is the expected decrease in K due to the presence of the surfactant monolayer. However, for the oleyl alcohol case, the clean and surfactant plots run essentially parallel to each other, while the stearic acid data shows (Fig. 3) a common x-intercept for the clean and surfactant data sets. Also, the decrease in K due to the introduction of oleyl alcohol is slightly smaller than for the stearic acid case. It is also noted that the behavior of the K versus g_p data is not as linear for the oleyl alcohol case as for the stearic acid case. This is particularly true for $g_p > 8g$, where the oleyl alcohol data flattens off. This point is further discussed below.

The data from Fig. 5 is plotted as a function of $\overline{S^2}$ in Fig. 6. Generally, the data tend to collapse as was the case for stearic acid. At $\overline{S^2} > 0.06$ m/m, the oleyl alcohol and clean data sets collapse completely. However, at $\overline{S^2} < 0.06$ m/m, K is slightly larger for the oleyl alcohol data than for the clean case. This

difference is small, and only slightly larger than the scatter and the two data sets are considered to fall on essentially the same line for the purposes of this work.

The region in Fig. 5 where the oleyl alcohol data flattens off occurs at $g_p > 8$g. This corresponds to the region $\overline{S^2} > 0.05$ m/m in Fig. 6, where a similar leveling-off is observed. The exact reason for this behavior is unclear. The fact that $\overline{S^2}$ increases with g_p in this region negates the possibility that the rubber dampers are absorbing the shaker's energy and preventing steeper waves from forming. Moreover, the possibility that in this region the gas exchange is too rapid for the pH electrode to follow is also not possible since the response time of the probe is much faster than that required to measure these CO_2 outgassing rates (as further evidenced by the much large values of K measured in Fig. 3). We suspect that the data is in fact linearly increasing in this regime, at perhaps a lower rate, but is being masked by the scatter. There is evidence for this in the existing data set. For example, if one considers the oleyl alcohol data in Fig. 6 in the region $0.02 < \overline{S^2} < 0.04$, the data appears flat, but is clearly part of an increasing trend when one considers the entire data set.

4 Discussion

The primary goal of this work was to extend the capillary wave results of Saylor and Handler (1997) to the more realistic case of surfactant covered capillary waves. These earlier experiments demonstrated, among other things, that millimeter scale capillary waves of moderate wave slope can result in relatively large gas exchange coefficients. In fact, K approached 0.01 cm/s which in a typical wind/wave tunnel experiment would not be achieved below a wind speed of 10 m/s. However, this earlier work did not reveal whether such large values of K would be observed, should surfactants be introduced into the system.

In the present investigation it is demonstrated that, at constant energy input to the tank, the presence of surfactants, both liquid phase and solid phase, reduced K. For stearic acid, this reduction approached a factor of two at $g_p = 3$ g as shown in Fig. 3. For oleyl alcohol as shown in Fig. 5, the reduction was slightly less than a factor of two and got smaller as g_p increased. This reduction in K is not surprising in light of the well-known wave damping properties of surfactants. What is of greater significance is that, even when the damping is at its largest, the values of K achieved in the surfactant covered experiments are not insignificant. For example, at $g_p = 3$ g, the presence of stearic acid reduces K to about 0.005 cm/s from 0.01 cm/s for the clean case. While this reduction is large, it is important to note that $K = 0.005$ cm/s is not achieved in typical wind/wave tunnel experiments below a wind speed $u \cong 7$ m/s (e.g Ocampo-Torres et al. 1994). Thus, these experiments demonstrate that even damped by surfactants, capillary waves have the potential to cause significant gas exchange.

Another goal of this work was to investigate the relationship between K and $\overline{S^2}$ for clean and surfactant covered capillary waves. This relationship is illustrated in Figs. 4 and 6 for stearic acid and oleyl alcohol, respectively, and shows that with or without the presence of surfactants, K can be approximated as a linear function of $\overline{S^2}$ with the possible exception of oleyl alcohol at $\overline{S^2} > 0.06$ m/m. More importantly, for both cases, the clean and surfactant data essentially fall on the same line, with the possible exception of stearic acid at large values of wave slope ($\overline{S^2} > 0.06$ m/m). Overall, then, Figs. 4 and 6 indicate that K is well-correlated by $\overline{S^2}$, supporting the idea that, for nonbreaking waves, knowledge of the statistics of the wave field is sufficient for predicting K. Moreover, these experiments were conducted at a higher wave number than that which was resolved in the work of Frew (1997), indicating that the excellent parameterization of K by $\overline{S^2}$ which was observed in that work should hold at even higher degrees of resolution. These results lend further credence to the ideas of Jähne et al. (1987), that air/sea gas exchange can be completely parameterized by $\overline{S^2}$. This is an important result from the perspective of remote sensing, since it is much easier to extrude wave slope statistics from optical or radar-based measurements, than other quantities which have been used to parameterize gas exchange in the past, such as wind speed or friction velocity.

The results reported here were all obtained using data from standing capillary waves. The natural question which arises is whether similar results would be obtained for progressive capillary waves. Szeri (1997) obtains an analytical relationship for gas exchange enhancement due to progressive capillary waves, based on the solution due to Crapper (1957). A plot of the variable describing gas exchange enhancement (the square root of Szeri's Eq. (3.2)) against $\overline{S^2}$ shows linear behavior for the range of $\overline{S^2}$ considered in this work ($\overline{S^2} < 0.1$). This observation suggests that a linear relationship between K and $\overline{S^2}$ may also exist for progressive capillary waves.

When interpreting the data obtained in these experiments, the possibility that factors other than pure capillary wave dynamics might be responsible for transport, was considered. For example, the possibility that acoustic streaming or some unrecognized tank vibration might be enhancing transport and inflating the measured values of K was a concern. To address this, rubber dampers were installed beneath the tank, as described in Sect. 2 to damp extraneous tank vibrations. In Fig. 7, the clean data from both facilities is plotted as a function of $\overline{S^2}$. The data for the facility with rubber dampers is slightly smaller than for the case without the rubber dampers. The difference, however, is comparable to the scatter in the data except at the highest value of $\overline{S^2}$. Thus, although the dampers significantly decrease the acoustic radiation emitted by the tank, the value of K does not change significantly, indicating that the measured gas exchange is caused by wave action and is only slightly affected by acoustic streaming or other tank vibrations. This point is further evidenced by the fact that the clean and surfactant data tend to collapse when plotted on K versus $\overline{S^2}$ coordinates (e.g. Fig. 4). At constant $\overline{S^2}$, the surfactant data is obtained at a higher g_p. Hence, the surfactant data is taken under conditions where more energy is being delivered to the tank than for the corresponding clean data point. Thus (again at constant $\overline{S^2}$), if acoustic streaming is present, the surfactant data experiences a greater amount of any such streaming than the clean data. The fact that the two data sets collapse suggests that these artifacts, if they exist at all, are not playing a significant role in the gas exchange process.

The question of whether the mean square slope due just to capillary waves $\overline{S_c^2}$ is the appropriate variable to parameterize K, or whether, as Jähne et al. (1987) contend, K must be parameterized by the mean square slope of the entire wave

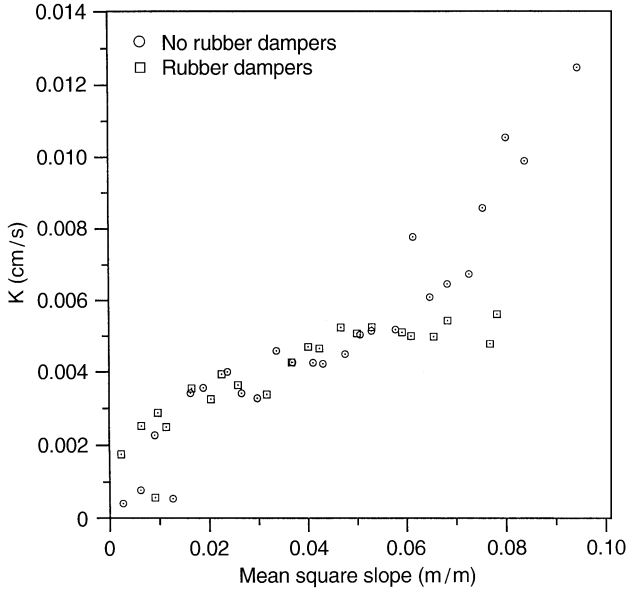

Fig. 7. K versus $\overline{S^2}$ for clean data only. Data is obtained with and without rubber dampers

spectrum, $\overline{S^2}$, is still on open question. Frew (1997) shows that $\overline{S^2}$ correlates the data well, and refers to unpublished data which suggests that the gas exchange coefficient is more linearly correlated to higher frequency waves; correlations to $\overline{S_c^2}$ are not presented. Back and McCready (1988) present simulations indicating a peak role for smaller waves, and Saylor (1988) comes to a similar conclusion. The present work indicates that small scale waves cause significant gas exchange, even when surfactants are present. While this points to an important role for capillary waves in gas exchange, it does not ascertain whether $\overline{S^2}$ or $\overline{S_c^2}$ is the variable most appropriate to parameterize K. Further work is necessary to address the spectral contribution of various bands of wave number to the gas exchange process.

Finally, a difference between the behavior of solid and liquid phase surfactants is noted. The K versus g_p data for stearic acid show significantly greater scatter than for the clean data (Fig. 3), or the oleyl alcohol data (Fig. 5). Experiments performed with stearic acid films made visible by talc, illustrated that this film can break, forming disconnected islands. Jähne et al. (1987) note 'breakage' of a stearic acid film in their wind/wave tunnel experiments. We postulate that, for the range of $\overline{S^2}$ explored here, the stearic acid monolayers are meta-stable, forming complete films in some experiments and breaking in others, resulting in greater scatter of the data. This scatter was not observed for oleyl alcohol, presumably because of the liquid nature of these monolayers.

5 Conclusions

The experiments presented here for capillary waves having a wavelength $\lambda = 2.87$ mm demonstrate that at constant energy input to the wave field, surfactants reduce the measured gas exchange coefficient. Peak reductions of about a factor of two were observed for both oleyl alcohol and stearic acid monolayers. These results notwithstanding, it is noted that even in the presence of surfactants, these capillary waves caused significant gas exchange, comparable to wind speeds of $u \approx 7$ m/s in typical wind/wave tunnel studies. The data for clean and surfactant cases collapsed onto a single line when plotted of K versus $\overline{S^2}$ coordinates, a result which has also been observed in wind/wave tunnel experiments. These results, obtained using oleyl alcohol and stearic acid, support the notion that knowledge of the statistics of the wave field is sufficient to predict the gas exchange coefficient, for the case of non-breaking waves. Further work is necessary before it can be determined if this is indeed the case in an actual oceanic environment. Of particular use would be studies utilizing natural ocean surfactants.

References

Adamson AW (1990) Physical Chemistry of Surfaces. New York: Wiley
Back DD; McCready MJ (1988) Effect of small-wavelength waves on gas transfer across the ocean surface. J Geophy Res 93: 5143–5152
Barger WR (1998) personal communication
Broecker HC; Petermann J; Siems W (1978) The influence of wind on CO_2-exchange in a wind-wave tunnel, including the effects of monolayers. J Mar Res 36: 595–610
Cox CS (1958) Measurements of slopes of high-frequency wind waves. J Mar Res 16: 199–225
Crapper GD (1957) An exact solution for progressive capillary waves of arbitrary amplitude. J Fluid Mech 2: 532–540
Dietrich G (1963) General Oceanography. New York: Wiley
Downing AL; Truesdale GA (1955) Some factors affecting the rate of solution of oxygen in water. J Appl Chem 5: 570–581
Faraday M (1831) On the forms and states assumed by fluids in contact with vibrating elastic surfaces. Philos Trans Roy Soc London 121: 319–340
Frew NM (1997) The role of organic films in air–sea gas exchange. In: The Sea Surface and Global Change. eds. Liss, P.S., Duce, R.A., pp 121–171, New York: Cambridge University Press
Frew NM (1998) personal communication
Gaines GL Jr (1966) Insoluble Monolayers at Liquid–Gas Interfaces. New York: Wiley
Hoover TE; Berkshire DC (1969) Effects of hydration on carbon dioxide exchange across an air–water interface. J Geophys Res 74: 456–464
Jähne B; Münnich KO; Siegenthaler U (1979) Measurements of gas exchange and momentum transfer in a circular wind-water tunnel. Tellus 31: 321–329
Jähne B; Münnich KO; Bösinger R; Dutzi A; Huber W; Libner P (1987) On the parameters influencing air–water gas exchange. J Geophys Res 92: 1937–1949
Kanwisher J (1963) On the exchange of gases between the atmosphere and the sea. Deep-Sea Res 10: 195–207
Liss PS (1973) Processes of gas exchange across an air–water interface. Deep-Sea Res 20: 221–238
MacIntyre F (1971) Enhancement of gas transfer by interfacial ripples. Phys Fluids 14: 1596–1604
Miles JW; Henderson DM (1990) Parametrically forced surface waves. Annu Rev Fluid Mech 22: 143–165
Ocampo-Torres FJ; Donelan MA; Merzi N; Jia F (1994) Laboratory measurements of mass transfer of carbon dioxide and water vapour for smooth and rough flow conditions. Tellus 46B: 16–32
Saylor JR; Handler RA (1997) Gas transport across an air/water interface populated with capillary waves. Phys Fluids 9: 2529–2541
Saylor JR (1998) The role of capillary waves in oceanic air/water gas exchange. Tellus 51B, in press
Stumm W; Morgan JJ (1970) Aquatic Chemistry. New York: Wiley
Szeri AJ (1997) Capillary waves and air–sea gas transfer. J Fluid Mech 332: 341–358
Witting J (1971) Effects of plane progressive irrotational waves on thermal boundary layers. J Fluid Mech 50: 321–334